WestVirginiaUniversity
THE RESEARCH REPOSITORY @ WVU

Faculty Scholarship

1988

Basis of strong change of hybridization-induced magnetic ordering between CeSb and CeTe

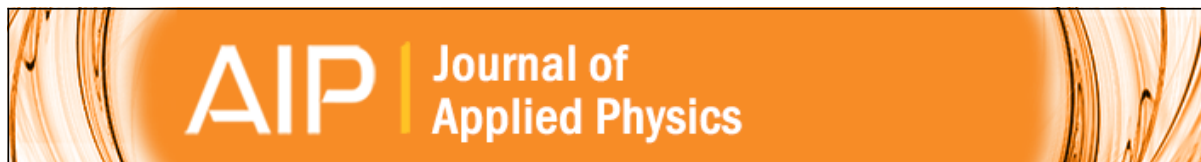N. Kioussis

B. R. Cooper

J. M. Wills

Follow this and additional works at: https://researchrepository.wvu.edu/faculty_publications

Basis of strong change of hybridization-induced magnetic ordering between CeSb and CeTe

N. Kioussis, B. R. Cooper, and J. M. Wills

Articles you may be interested in

Strong magnetic fluctuations in transition metal oxides (invited)
J. Appl. Phys. **79**, 5023 (1996); 10.1063/1.361564

Kinetics of ordering in the percolation magnet
AIP Conf. Proc. **256**, 433 (1992); 10.1063/1.42346

The role of orbital polarization and correlation effects in the magneto-optic behavior of CeSb and CeTe
J. Appl. Phys. **70**, 5809 (1991); 10.1063/1.350144

Pressure-induced electrical and magnetic properties in CeAs, CeSb and CeBi
J. Appl. Phys. **69**, 4696 (1991); 10.1063/1.348301

Magnetic excitations in ferromagnetic CeSb
J. Appl. Phys. **50**, 2040 (1979); 10.1063/1.327101

Basis of strong change of hybridization-induced magnetic ordering between CeSb and CeTe

N. Kioussis[a] and B. R. Cooper
Department of Physics, West Virginia University Morgantown, West Virginia 26506

J. M. Wills
Los Alamos National Laboratory, Los Alamos, New Mexico 87545

A sharp change in the nature of the magnetic ordering has been observed on going from CeSb to CeTe, both of which have NaCl structures with a small decrease in lattice parameter. This is an interesting example of the way in which hybridization of partially delocalized f electrons with band electrons gives rise to highly unusual magnetic properties which show great chemical sensitivity. In the present paper we apply our previous *ab initio* treatment of hybridization-induced effects to investigate this striking change in magnetic behavior. We have performed self-consistent warped muffin-tin LMTO band calculations treating the Ce $4f$ states as resonance states that are constrained to be localized. Compared to CeSb, the anion-derived p bands in CeTe sink well below the Fermi energy, thus strongly changing the band-f hybridization. We have calculated the hybridization dressing of the crystal-field levels and the anisotropic two-ion exchange interaction and compared them with those calculated for CeSb and with experiment. A strong decrease in the two-ion interaction explains the drastic change in observed magnetic behavior between CeSb and CeTe.

I. INTRODUCTION

Among the NaCl-structure monopnictides and mono-chalcogenides of cerium, CeSb exhibits the most unusual magnetic behavior.[1] The most striking feature of its low-field phase diagram is the occurrence of high-temperature ($8.5 < T < T_N \simeq 16.2$ K) phases consisting of a periodic sequence of nonmagnetic and magnetically ordered (001) planes with up or down moments along the [001] cube edge and close to saturation ($\sim 2.1\mu_B$). The nonmagnetic planes, which are actually paramagnetic in nature,[1] disappear below 8.5 K yielding a type-IA antiferromagnetic structure.

The unique magnetic properties of CeSb are very sensitive to any perturbation such as pressure,[1] the dilution[2] of cerium by nonmagnetic Y or La, or the substitution of antimony by another pnictogen[3] (Bi, As), or by tellurium.[1,4] In particular, magnetization[1,4] and neutron scattering[1] experiments on $CeSb_{1-x}Te_x$ have shown that for a Te concentration as small as $x = 0.02$, the Néel temperature drops abruptly from 16 K to less than 4 K, and the nonmagnetic planes are supressed. Moreover, the crystal-field (CF) splitting between the ground-state Γ_7 doublet and the Γ_8 quartet of the $4f_{5/2}$ multiplet, which is about 37 K in CeSb, increases with tellurium concentration, reaching its maximum value of about 105 K at $x = 0.5$, and the decreases monotonically with further increase of x to the value of about 32 K in[1] CeTe. CeTe orders at[5,6] $T_N \simeq 2.2$ K into a type-IA antiferromagnetic structure, with a Ce^{3+} local moment of only $0.2\mu_B$ aligned along the $\langle 111 \rangle$ direction, in sharp contrast with CeSb. This dramatic change in magnetic behavior on going from CeSb to CeTe with little change in the lattice constant, and where the only obvious change is the addition of an anion p electron, clearly demonstrates the sensitivity of the hybridization-mediated exchange interactions to chemical environment.

The large cube-edge anisotropy and consequent unusual magnetic behavior of the heavier cerium monopnictides (CeSb and CeBi) have been successfully explained[7–9] on the basis of an anisotropic hybridization-mediated two-ion interaction. This interaction arises through cooperative hybridization between moderately delocalized f electrons of the Ce^{3+} lattice and band electrons of non-f atomic parentage. However, until recently, the basic parameters entering the theory, namely, the anisotropic two-ion exchange interactions and the CF splitting, had been taken as phenomenological input to match the experimentally observed Néel temperature, low-temperature moment, and CF splitting. Recently, Wills and Cooper[10] have presented a first-principles calculation of the model parameters for the cerium monopnictides, based on self-consistent, warped muffin-tin, LMTO band structures calculated for these compounds. The purpose of this paper is to evaluate from first principles the model parameters for CeTe in order to understand quantitatively the origins of the variation of the hybridization-induced anisotropies on going from a weakly hybridizing system such as CeSb to the presumably more strongly hybridizing CeTe system, which being at the border between a magnetic and a nonmagnetic state has sometimes been referred to[1] as a dense Kondo system.

II. THE METHOD

The first step is the generation of a self-consistent one-electron potential describing the band structure of CeTe. This is obtained from a warped muffin-tin LMTO band-structure calculation, without recourse to the atomic sphere approximation,[11] i.e., using a nonzero tail parameter as a variational parameter. The full interstitial potential is used,

---

[a] Present address: Department of Physics, California State University at Northridge, Northridge, CA 91330.

and the only shape approximation to the potential is a spherical averaging in nonoverlapping muffin-tin spheres surrounding the Ce and Te sites. The potential is evaluated at the experimental volume, and the radii of the muffin-tin spheres are chosen to make the potential continuous where spheres touch.

The core states are included self-consistently and are obtained from the Dirac equation for the spherically averaged potential at each site. The Ce f electrons are treated as localized rather than itinerant states and thus they are included self-consistently as core states at each iteration, not being allowed to hybridize with band states. Thus as each iteration these $4f$ states are treated as resonant states that are constrained to be localized.[10] The radial basis functions for the (non-f) bands within the muffin-tin spheres are solutions of the scalar relativistic radial equation.[12] Spin-orbit coupling is included self-consistently. The band structure is divided into three energy windows: the semicore Ce $5p$ and Te $5s$ bands are calculated with an imaginary LMTO tail parameter κ, with κ^2 equal to -0.9 and -0.3 Ryd, respectively; and the Ce valence $6s$, $6p$, and $5d$ states and Te valence $5p$ states are calculated with a $\kappa^2 = 0.23$ Ryd, which is the average energy over occupied states in the interstitial.

We next calculate the basic model parameters entering the Anderson (Coqblin–Schrieffer) model Hamiltonian.[13] These are the band energies, ϵ_{nk}; the band f hybridization matrix element, $V_{nk,m}$ of the Hamiltonian for a single-particle potential surrounding the Ce site between the band state $|n,\mathbf{k}\rangle$ and the Ce$|5/2,m\rangle$ state; the f-state energy, E_f, with respect to the band Fermi energy E_F; and finally the intra-atomic f-f correlation energy U. Because accurate determination of these quantities requires a highly accurate representation of the bands around the resonant f-state energy, we perform a final band calculation, after the self-consistency process, with the tail parameter of the highest-energy window set equal to the resonant f-state energy.

Identifying the Ce $4f_{5/2}$ state with the $l = 3, j = 5/2$ resonance in the local potential within a Ce muffin tin and projecting band-f overlap out of the matrix element to correct for band-f nonorthogonality, the hybridization potential matrix elements $V_{nk,m}$ have been shown[10] to be the product of two quantities. The first of these is the hybridization potential, which is proportional to the resonance width Γ, and which provides an overall scale. The second of these is proportional to the product of the KKR structure function and the LMTO eigenvectors, and describes the details of the band structure. The energy necessary to place the Ce f electron in a band state at the Fermi level, $E_F - E_f$, and the energy required to change from an f^1 configuration to an f^2 configuration, $E_f + U - E_F$, are obtained from self-consistent local-density supercell calculations, in which one considers eight atoms per unit cell as opposed to two for the ground-state calculation. These energies are obtained by removing (adding) an f electron to the central Ce site and allowing the system to relax, resulting in a d screening (antiscreening) of the f hole (electron).[14] We find that $E_F - E_f = 3$ eV, in good agreement with the value of 2.6 ± 0.1 eV found in x-ray photoemission experiments,[15] and $U = 6.3$ eV.

The hybridization-induced shift in the crystal-field energy levels, ΔE_M, in the paramagnetic phase is calculated by applying the Schrieffer–Wolff[16] transformation to the CS Hamiltonian to order $(V_{nk,m})^2$; and the hybridization-mediated two-ion interactions are determined[10] by applying the Schrieffer–Wolff transformation to order $(V_{nk,m})^4$ and treating the exchange scattering Hamiltonian in second-order perturbation theory on band states. There are two contributions to ΔE_M: a negative contribution resulting from hybridization of band states above E_F with the Cef^1 state below E_F, and a second positive contribution (which is, however, smaller by a factor of $1/U$ relative to the first one) resulting from hybridization of band states below E_F with the Ce f^2 state above E_F.

III. NUMERICAL RESULTS AND DISCUSSION

The band structure of CeTe is plotted in Fig. 1. The energy of the corelike Ce $4f_{5/2}$ state lies 78 mRyd below the Fermi energy. At Γ, the Te p-derived bands have $\Gamma_8^{(-)}$ symmetry while the Ce d-derived bands are the bases for three representations, one with $\Gamma_7^{(+)}$ and two with $\Gamma_8^{(+)}$ symmetry. It is important to note that on going from CeSb to CeTe, the addition of an anion p electron has caused the p-derived bands to sink far below the Fermi level, so that the bands dominating the hybridization-induced properties in CeTe in the vicinity of Γ are largely derived from the Ce $5d$ states.

The total density of states (solid curve) corresponding to the band structure in Fig. 1 is shown in Fig. 2. Also plotted in the same figure are the partial density of states for the Ce d-derived (short-dashed curve) and the Te p-derived (long-dashed curve) bands, respectively. The Fermi energy and the density of states at the Fermi energy in CeTe are 0.475 Ryd and 15.6 states/Ryd, respectively, compared to the corresponding values of 0.374 Ryd and 4.4 states/Ryd in CeSb, indicating the metallic and semimetallic character of these compounds, respectively. However, aside from the location of E_F and the consequent density of states at E_F, and the opening of a gap in the density of states in CeTe below E_F between 0.325 and 0.375 Ryd, the density of states for the two compounds are qualitatively similar.

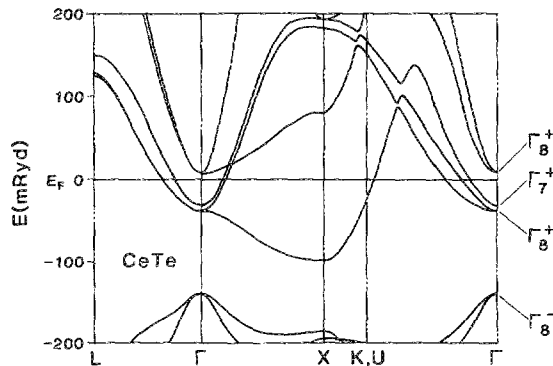In both compounds, the hybridization-induced shift,

FIG. 1. Warped-muffin-tin LMTO band structure of CeTe along symmetry lines of the fcc Brillouin zone with the Ce $4f$ states treated as localized (see text). Energies are relative to the Fermi energy.
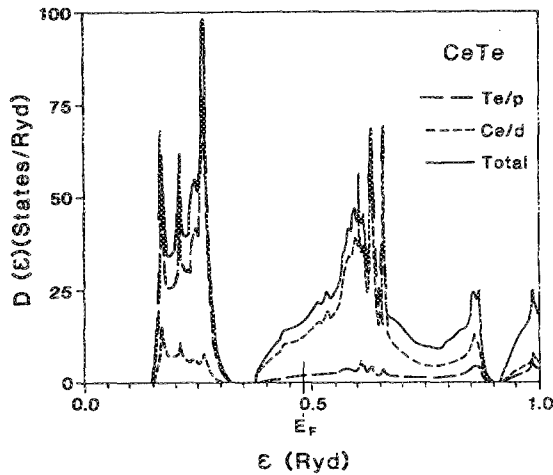
FIG. 2. Total density of states (solid curve) of the LMTO band structure of CeTe corresponding to the band structure in Fig. 1. Also shown are the partial density of states for the Ce d-derived (short-dashed curve) and Te p-derived (long-dashed curve) bands, respectively. The Fermi energy is at 0.475 Ryd.

δE_{Γ_8}, in the bare crystal-field energy level of the Γ_8 quartet is found to be larger than the corresponding shift, δE_{Γ_7}, of the Γ_7 doublet, by approximately a factor of 2. This results[10] from the fact that the set of degenerate bands belonging to the star of a general point in the irreducible wedge of the Brillouin zone form a basis for a representation of the cubic group that contains the Γ_7 representation twice and the Γ_8 representation four times. Importantly, the positive contributions to δE_{Γ_7} and δE_{Γ_8} resulting from hybridization of band states below the Fermi with the f^2 state are about the same in both CeTe and CeSb. On the other hand, the negative dominant contribution to δE_{Γ_7} and δE_{Γ_8} resulting from hybridization of band states above the Fermi energy with the f^1 state decreases by about a factor of 2 on going from CeSb to CeTe. This arises from the fact that the hole band states in CeSb in the vicinity of its Fermi energy, which were yielding the largest negative contribution to δE, become occupied on going to CeTe, thus giving a positive contribution, which, however, is reduced by a factor of $1/U$. Furthermore, the large cancellation between the positive and negative term, which are of comparable magnitude, results in a net shift, $\delta E_{CF} = \delta E_{\Gamma_8} - \delta E_{\Gamma_7}$, of 45 K in CeTe compared to the corresponding value of 194 K in CeSb. However, in the absence as yet of a value for the "bare" (without hybridization dressing) CF splitting for CeTe, it is rather difficult to make a direct comparison of theory and experiment as in the case of CeSb, where the agreement was found to be excellent.[10]

Finally, of most immediate interest, we have calculated the hybridization-mediated exchange interactions,[7,8] $E_n^{mm'}$, between two nth nearest-neighbor Ce^{3+} ions (where m and m' denote the components of the angular momentum quan-

tized along the interionic axis) which are pertinent to the dramatic change in magnetic behavior on going from CeSb to CeTe. We find that as in the case of[10] CeSb, the dominant matrix elements involve the $m,m = \pm 1/2$ states, which correspond to the piling up of charge along the interionic axis. In particular, for $m,m' = \pm 1/2$ we find that E_1, which in the phenomenological treatment[7-9] is chosen to match the Néel temperature, decreases from 0.84 K in CeSb to 0.15 K in CeTe, yielding a ratio of about 5.7, in good agreement with the value of 7 for the ratio of the experimentally observed Néel temperatures. Moreover, for $m,m' = \pm 1/2$ we find that $E_2 = 3.1E_2$ (ferromagnetic) in CeSb compared to $0.42E_1$ (antiferromagnetic) in CeTe; and $E_3 = -0.02E_1$ in CeSb compared to $0.17E_1$ in CeTe. This occurrence of ferromagnetic and antiferromagnetic interactions of comparable strength, and the consequent need for "compromise" might be responsible for the low moment value in CeTe rather than a "Kondo effect," and also for the change in magnetic structure compared to that of CeSb. The inclusion of all the transition channels of the range function matrix in the phenomenological theory to treat in detail the magnetic ordering in these compounds is currently under investigation.

ACKNOWLEDGMENTS

[1] J. Rossat-Mignod, J. M. Effantin, P. Burlet, T. Chattopadhyay, L. P. Regnault, H. Bartholin, C. Vettier, O. Vogt, D. Ravot, and J. C. Achart, J. Magn. Magn. Mater. 52, 111 (1985).
[2] B. R. Cooper and O. Vogt, J. Phys. (Paris) 32, C1-1026 (1971).
[3] H. Bartholin, O. Vogt, and J. P. Senateur, J. Magn. Magn. Mater. 15–18, 1247 (1980).
[4] D. Ravot, A. Mauger, J. C. Achard, M. Bartholin, and J. Rossat-Mignod, Phys. Rev. B 28, 4558 (1983).
[5] F. Hulliger, B. Natterer, and H. R. Ott, J. Magn. Magn. Mater. 8, 87 (1978); H. R. Ott, J. K. Kjems, and F. Hulliger, Phys. Rev. Lett. 42, 1378 (1979).
[6] D. Ravot, P. Burlet, J. Rossat-Mignod, and J. L. Tholence, J. Phys. (Paris) 41, 1117 (1980).
[7] R. Siemann and B. R. Cooper, Phys. Rev. Lett. 44, 1015 (1980).
[8] B. R. Cooper, R. Siemann, D. Yang, P. Thayamballi, and A. Banerjea, in The Handbook of the Physics and Chemistry of the Actinides, edited by A. J. Freeman and G. G. Lander (North-Holland, Amsterdam, 1985), Vol. 2, Chap. 6, pp. 435–500.
[9] N. Kioussis, B. R. Cooper, and A. Banerjea, J. Appl. Phys. 61, 3388 (1987).
[10] J. M. Wills and B. R. Cooper, Phys. Rev. 36, 3809 (1987).
[11] H. L. Skriver, The LMTO Method (Springer, Berlin, 1984).
[12] D. D. Koelling and B. N. Harmon, J. Phys. C 10, 3107 (1977).
[13] B. Coqblin and J. R. Schrieffer, Phys. Rev. 185, 847 (1969).
[14] M. R. Norman, D. D. Koelling, A. J. Freeman, H. J. F. Jansen, B. I. Min, T. Oguchi, and L. Ye, Phys Rev. Lett. 53, 1673 (1984).
[15] W. Gudat, M. Campagna, R. Rosei, J. H. Weaver, W. Eberhardt, F. Hulliger, and E. Kaldis, J. Appl. Phys. 52, 2123 (1981).
[16] J. R. Schrieffer and P. A. Wolff, Phys. Rev. 149, 491 (1966).